Available online at www.sciencedirect.com
SCIENCE DIRECT®
International Journal of Heat and Mass Transfer 49 (2006) 2158–2172
International Journal of HEAT and MASS TRANSFER
www.elsevier.com/locate/ijhmt

Influence of Lewis number on strain rate effects in turbulent premixed flame propagation

Nilanjan Chakraborty [a], R.S. Cant [b,*]

[a] Liverpool University, Engineering Department, Brownlow Hill, Liverpool L69 3GH, UK
[b] Cambridge University, Engineering Department, Trumpington Street, Cambridge CB2 1PZ, UK

Received 25 September 2005; received in revised form 23 November 2005
Available online 28 February 2006

Abstract

The effects of tangential strain rate on the displacement speed of turbulent premixed flames in the thin reaction zones regime are studied for three different Lewis numbers ($Le = 0.8$, 1.0 and 1.2) using three-dimensional compressible direct numerical simulation (DNS) of statistically planar flames. For non-unity Lewis numbers it is shown that the variations of temperature and scalar gradient in response to tangential strain rate on a given reaction progress variable isosurface have a profound influence on displacement speed behaviour. In the case of $Le = 0.8$, temperature and tangential strain rate are found to be positively correlated at locations of zero curvature whereas the opposite behaviour is apparent for the case of $Le = 1.2$. It is demonstrated that the effects of the temperature-curvature and tangential strain rate-curvature correlations are implicitly present in the response of the temperature to local strain rate. The temperature-curvature correlation and strain rate-curvature correlation are found to be in agreement with previous experimental results. Displacement speed and strain rate are found to be weakly correlated in general, but their conditional joint pdf at zero curvature locations shows a negative correlation.

Keywords: Lewis number; Tangential strain rate; Displacement speed; Direct numerical simulation (DNS); Surface density function (SDF)

1. Introduction

Lewis number (Le) is defined as the ratio of thermal diffusivity to species diffusivity. In a real premixed flame it is difficult to define a single unique Lewis number for the whole combustion process because of the presence of many different species with different thermo-physical properties. In order to simplify the analysis, a premixed flame is often characterised by the Lewis number of the deficient reactant [1]. A number of previous numerical and theoretical studies have used such a definition of Lewis number in order to analyse the effects of differential diffusion in turbulent premixed flames [1–8].

Asymptotic analysis [1] has been employed to understand the effects of differential diffusion on premixed flame propagation in the corrugated flamelets regime [9]. Sivashinsky [2] analysed differential diffusion effects from the point of view of flame-stability in non-unity Lewis number flames. Experimental studies were carried out by Libby et al. [3] who reported the influence of non-unity Lewis number on strain rate effects in premixed flame propagation, and by Abdel-Gayed et al. [4] who studied the effects of Lewis number on the turbulent burning velocity. Numerical simulations [5–8] have been employed to address the issue of differential diffusion from a number of different aspects. Ashurst et al. [5] studied the effects of non-unity Lewis number on global flame structure using two-dimensional direct numerical simulation (DNS) with single step chemistry, while Haworth and Poinsot [6] using similar techniques presented the strain-curvature correlation for non-unity Lewis number. The turbulent flame propagation speed at non-unity Lewis number was investigated by Trouvé and Poinsot [7] based on three-dimensional

* Corresponding author. Tel.: +44 1223 339 722; fax: +44 1223 332 662.
E-mail address: rsc10@eng.cam.ac.uk (R.S. Cant).

0017-9310/$ - see front matter © 2006 Elsevier Ltd. All rights reserved.
doi:10.1016/j.ijheatmasstransfer.2005.11.025

Nomenclature

a_T	flame tangential strain rate
a_0	acoustic speed in fresh gas
c	reaction progress variable
c^*	progress variable value defining flame surface
C_P	reference specific heat at constant pressure
C_V	reference specific heat at constant volume
D	progress variable diffusivity
Da	Damköhler number
E	non-dimensional internal energy
H	heat of the reaction per unit mass of mixture
k	turbulent kinetic energy
l_0	reference length scale
L	length of the computational domain
Le	Lewis number
Ma	Mach number
$\vec{N}$	local flame normal vector
P	non-dimensional pressure
Pr	Prandtl number
q_k	heat flux in kth direction
R	specific gas constant
Re	Reynolds number for non-dimensionalising of the momentum equations
Re_t	turbulent Reynolds number
Sc	Schmidt number
S_d	local flame displacement speed
S_L	laminar flame speed
S_n	normal diffusion component of displacement speed
S_r	reaction component of displacement speed
S_t	tangential diffusion component of displacement speed
t	non-dimensional time
T	non-dimensional temperature
T_{ad}	adiabatic flame temperature
T_0	reactant temperature
$\widehat{T}$	instantaneous dimensional temperature
$\vec{u}$	non-dimensional fluid velocity vector
u_i	ith component of non-dimensional fluid velocity
u_0	reference velocity scale
u'	non-dimensional initial root mean square fluctuation velocity
$\dot{w}$	chemical reaction rate
x_i	ith Cartesian co-ordinate

Greek symbols

α	heat release factor
β	Zel'dovich number
γ	ratio of specific heats
δ_L	laminar flame thickness
η	Kolmogorov length scale
κ_m	mean curvature of the flame
λ	thermal conductivity
λ_0	reference thermal conductivity
μ	dynamic viscosity
ρ	density
ρ_0	reactant density, reference density
σ	surface density function (SDF)
τ	heat release parameter
τ_c	chemical time scale
τ_{f0}	initial turbulent eddy turn-over time/flow time scale
τ_{ij}	viscous stress

compressible DNS, and the effects of differential diffusion on the global behaviour of flame displacement speed were addressed, but the effects of curvature and strain rate on local displacement speed were not considered. Rutland and Trouvé [8] addressed the effects of tangential strain rate on the local rate of burning in the corrugated flamelets regime, but the analysis was focussed on fuel consumption rates rather than on local flame propagation. Im and Chen [10] demonstrated the influence of differential diffusion on local stretch effects in flame propagation behaviour using two-dimensional DNS of H_2-air flames with detailed chemistry. Recently, Shamim [11] investigated the effects of non-unity Lewis number on turbulent diffusion flames under small strain rates. Hilbert and Thévenin [12] investigated the effects of non-unity Lewis number on the maximum temperature attained in non-premixed flames.

Tangential strain rate is an important quantity, which significantly affects flame propagation. Since the tangential strain rate acting on a flame surface is dependent on the local flame geometry, it is to be expected that tangential strain rate and flame curvature should be interrelated [13]. In the case of non-unity Lewis numbers the effects of tangential strain rate on temperature variation on an isosurface of reaction progress variable significantly affects the local chemical reaction rate [3,8]. Moreover, the correlation between tangential strain rate and curvature affects the local temperature–strain rate correlation, which in turn affects the strain rate response of flame displacement speed. For adiabatic, low Mach number, unity Lewis number flames the non-dimensional temperature is equal to the reaction progress variable, which makes the temperature distribution uniform on a given progress variable isosurface. As a result of this, the reaction rate also becomes uniform on a given isosurface, which makes the flame relatively insensitive to stretch effects induced by the tangential strain rate.

By contrast, for non-unity Lewis number flames, it has been found that curvature effects on flame propagation are much greater than for unity Lewis number flames, due to significant temperature variations within reaction progress variable isosurfaces. In the thin reaction zones

regime it is known that curvature effects dominate over laminar propagation effects [9] so it is expected that tangential strain rate effects on flame propagation will be significant in this regime due to the existence of a non-zero strain rate-curvature correlation. In the thin reaction zones regime, the Karlovitz number is high ($Ka > 1$) and the Damköhler number is smaller than is found in the corrugated flamelets regime ($Da \leqslant 1$). In this situation the flow timescale is small compared to the chemical timescale, and so the flame cannot respond quickly to hydrodynamic perturbations and maintain its original structure [8]. This indicates that it is important to address strain rate effects on flame propagation for non-unity Lewis numbers in the thin reaction zones regime.

The displacement speed of a reaction progress variable isosurface is defined as the speed at which the surface moves normal to itself relative to the initially coincident material surface. Displacement speed is an important quantity since it appears in the governing equations for both the flame surface density (FSD) [13,14] and the level set (G equation) [9] modelling approaches. In the present study, the effects of tangential strain rate on displacement speed in the thin reaction zones regime are addressed based on three-dimensional compressible DNS of statistically planar turbulent premixed flames. Curvature effects on displacement speed are kept beyond the scope of the present work and are discussed elsewhere [15]. The main objectives of the present paper are twofold:

1. Understanding of the influences of differential diffusion on displacement speed behaviour in response to tangential strain rate, based on three-dimensional DNS with simplified chemistry.
2. Assessment of the modelling arguments of Peters [9] for the thin reaction zones regime which were based on two-dimensional DNS with detailed chemistry.

In the present study, three different DNS datasets are considered having Lewis numbers $Le = 0.8$, 1.0 and 1.2 respectively. Joint pdfs of temperature and strain rate are presented together with the corresponding conditional joint pdfs at zero curvature locations. The temperature statistics are found to be consistent with previous DNS [8] and experimental studies [3]. Local effects of tangential strain rate on displacement speed and its components are presented in terms of their joint pdfs and also in terms of conditional joint pdfs at zero curvature locations in order to understand the effect of tangential strain rate in isolation. Strain rate effects arising from purely fluid-dynamical interactions, even in the absence of complex chemistry, show qualitative trends similar to those observed in previous two-dimensional DNS studies with detailed chemistry [16,17]. This is believed to be the first comprehensive analysis where strain rate effects on displacement speed at non-unity Lewis number have been studied in isolation. The results are likely to be of particular significance for flame propagation modelling in the thin reaction zones regime.

Section 2 of this paper provides the necessary mathematical background, and the numerical implementation is presented briefly in Section 3. Results for the effects of Lewis number on displacement speed in relation to tangential strain rate are presented and subsequently discussed in Section 4. Finally, Section 5 summarises the findings.

2. Mathematical modelling

Ideally, combustion DNS should incorporate detailed chemistry as well as the three-dimensionality of the turbulent flow field. In practice, limitations of computer capacity mean that DNS of turbulent flames must be carried out either in two dimensions with detailed chemistry or in three dimensions with simplified chemistry. The latter approach is adopted here, using a single step irreversible Arrhenius type chemical reaction, and a single reaction progress variable (c) which increases monotonically from zero in reactants to unity in fully burned products. The reaction progress variable can be defined in terms of deficient reactant mass fraction as:

$$c = \frac{Y_{\mathrm{R}0} - Y_{\mathrm{R}}}{Y_{\mathrm{R}0} - Y_{\mathrm{R}\infty}} \tag{1}$$

where subscript 0 and ∞ are used respectively to denote values in fresh gases and fully burned products. The transport equation for the reaction progress variable is given by:

$$\rho\frac{\partial c}{\partial t} + \rho u_j \frac{\partial c}{\partial x_j} = \dot{w} + \frac{\partial}{\partial x_j}\left[\rho D \frac{\partial c}{\partial x_j}\right] \tag{2}$$

where $\dot{w}$ is the chemical reaction rate and D is the diffusivity. The chemical reaction rate for fuel–lean mixtures can be written as:

$$\dot{w} = B^*\rho(1-c)\exp\left[-\frac{\beta(1-T)}{1-\alpha(1-T)}\right] \tag{3}$$

where B^* is the pre-exponential factor, α is the heat release parameter, β is the Zel'dovich factor and T is non-dimensional temperature given by:

$$T = (\widehat{T} - T_0)/(T_{\mathrm{ad}} - T_0) \tag{4}$$

where $\widehat{T}$ is the dimensional temperature, T_0 is the initial temperature and T_{ad} is the adiabatic flame temperature. The heat release parameter is α and τ are defined as:

$$\alpha = (T_{\mathrm{ad}} - T_0)/T_{\mathrm{ad}}, \qquad \tau = (T_{\mathrm{ad}} - T_0)/T_0 \tag{5}$$

It is useful for the sake of completeness to present the energy equation

$$\frac{\partial \rho E}{\partial t} + \frac{\partial}{\partial x_k}\rho u_k E = -\frac{\partial}{\partial x_k}u_k P + \frac{\partial}{\partial x_i}\tau_{ki}u_i - \frac{\partial}{\partial x_k}q_k \tag{6i}$$

where E is stagnation internal energy given by:

$$E = C_V\widehat{T} + (1/2)u_k u_k + H(1-c) \tag{6ii}$$

in which C_V is the specific heat at constant volume and H is the heat of reaction per unit mass of reactants. In Eq. (5) τ_{ki}

and q_k are the viscous shear stress and heat flux respectively, and are given by:

$$\tau_{ki} = \mu\left(\frac{\partial u_i}{\partial x_j} + \frac{\partial u_j}{\partial x_i}\right) - \frac{2}{3}\mu\delta_{ij}\frac{\partial u_k}{\partial x_k} \tag{6iii}$$

$$q_k = -\lambda(\partial\widehat{T}/\partial x_k) + \rho DH(\partial c/\partial x_k) \tag{6iv}$$

where μ is the viscosity and λ is the thermal conductivity. It is evident from Eqs. (2), (3) and (6) that the relative strength of thermal and mass diffusivity plays an important role in heat and mass transport. The ratio of thermal diffusivity to species diffusivity is the Lewis number defined as:

$$Le = \lambda/(\rho C_P D) \tag{7}$$

where C_P is the specific heat at constant pressure. In the present study λ, μ, C_P, C_V and ρD are taken to be independent of temperature. This ensures that the representative value of Le does not change during the combustion process.

The reaction progress variable transport equation can be rewritten in kinematic form for an isosurface $c = c^*$ as [16]:

$$\left.\frac{\partial c}{\partial t}\right|_{c=c^*} + u_j\left.\frac{\partial c}{\partial x_j}\right|_{c=c^*} = S_{\mathrm{d}}|\nabla c||_{c=c^*} \tag{8}$$

where S_{d} is the displacement speed of the $c = c^*$ isosurface given by:

$$S_{\mathrm{d}} = \left.\frac{\dot{w} + \nabla\cdot(\rho D\nabla c)}{\rho|\nabla c|}\right|_{c=c^*} \tag{9i}$$

The displacement speed S_{d} is made up of three components [18]:

$$S_{\mathrm{d}} = S_{\mathrm{r}} + S_{\mathrm{n}} + S_{\mathrm{t}} \tag{9ii}$$

where the reaction component is:

$$S_{\mathrm{r}} = \left.\frac{\dot{w}}{\rho|\nabla c|}\right|_{c=c^*} \tag{9iii}$$

the normal diffusion component is:

$$S_{\mathrm{n}} = \left.\frac{\vec{N}\cdot\nabla(\rho\mathrm{D}\vec{N}\cdot\nabla c)}{\rho|\nabla c|}\right|_{c=c^*} \tag{9iv}$$

and the tangential diffusion component is:

$$S_{\mathrm{n}} = -2D\kappa_{\mathrm{m}} \tag{9v}$$

where $\vec{N}$ is local flame normal vector defined as: $\vec{N} = -\nabla c/|\nabla c||_{c=c^*}$ and κ_{m} is the local mean flame curvature given by: $\kappa_{\mathrm{m}} = (1/2)\nabla\cdot\vec{N}|_{c=c^*}$. According to this convention the flame normal vector points towards the reactants and flame surface curved convex towards the reactants is assumed to have positive curvature. The tangential strain rate a_{T} acting on a $c = c^*$ isosurface is defined as:

$$a_{\mathrm{T}} = (\delta_{ij} - N_iN_j)\left.\frac{\partial u_i}{\partial x_j}\right|_{c=c^*} \tag{10}$$

It is evident from Eqs. (9) and (10) that the displacement speed and tangential strain rate are both strongly dependent on local flame geometry. Since flame curvature is representative of local flame geometry it can be expected that curvature effects implicitly play an important role in the response of the displacement speed to local tangential strain rate.

3. Numerical implementation

DNS has been carried out for statistically planar flames in a cubical domain where two of the opposing faces in the direction of mean flame propagation are taken to be partially non-reflecting boundaries, and the remaining transverse faces are taken to be periodic boundaries. A similar configuration has proved highly effective in many previous combustion DNS studies [10,16–19]. The Navier–Stokes Characteristic Boundary Condition (NSCBC) formalism [20] is used to specify the partially non-reflecting boundary conditions. The initial turbulent velocity field is generated using a Batchelor–Townsend spectrum [21] with the help of a pseudo-spectral method [22]. The flame is initialised by a steady state planar unstrained laminar flame solution. Spatial discretisation is carried out using an explicit 10th order central difference scheme [23] in the interior, reducing gradually to a 4th order one-sided explicit difference as the inlet and outlet boundaries are approached. Time advancement is carried out using a third order low storage Runge–Kutta scheme [24].

The DNS grid spacing is determined by the requirement to resolve the structure of the flame. In the present case the laminar flame thickness is defined based on species mass fraction after Echekki and Chen [16]:

$$\delta_{\mathrm{L}} = 1/(\max|\partial c/\partial n|) \tag{11}$$

For completeness it is worth mentioning that the thermal flame thickness is defined as $\delta_{\mathrm{th}} = (T_{\mathrm{ad}} - T_0)/\max|\partial\widehat{T}/\partial n|$. For all cases about 10 grid points are kept within both δ_{L} and δ_{th}.

4. Results and discussion

The thermo-physical and numerical parameters for the present study are presented in Tables 1 and 2 respectively. For all three Lewis number cases considered, the same initial turbulence flow field is used in order to keep the same turbulence intensity u'/S_{L} and the same ratio l/δ_{th} of integral length scale to flame thermal thickness. The ratio l/δ_{L} is slightly different for the three Lewis number cases

Table 1
Thermo-physical parameters used for all simulations

Ratio of specific heat ($\gamma = C_P/C_V$)	1.4
Heat release parameter, τ	3.0
Zel'dovich number, β	6.0
Reynolds number, $Re = \rho_0 S_{\mathrm{L}} l_0/\mu$	25.0
Mach number, $Ma = S_{\mathrm{L}}/a_0$	0.014159

The domain length is l_0 and the speed of sound in fresh gas is a_0.

Table 2
Length scale parameters

Numerical parameter	$Le = 0.8$	$Le = 1.0$	$Le = 1.2$
DNS grid size	96^3	96^3	96^3
Normalised grid spacing, $\Delta x/l_0$	0.0105	0.0105	0.0105
Initial turbulence intensity, u'/S_L	7.1907	7.1907	7.1907
Laminar flame thickness, $\delta_L = 1.0/\max(\lvert\partial c/\partial n\rvert)$	$0.1182l_0$	$0.1038l_0$	$0.0926l_0$
Thermal thickness, $\delta_T = (T_{ad} - T_0)/\max(\lvert\partial \widehat{T}/\partial n\rvert)$	$0.1038l_0$	$0.1038l_0$	$0.1038l_0$
Initial integral length scale to flame thickness ratio, l/δ_L	1.70	1.92	2.24
Initial turbulent Reynolds number, $\rho_0 u' l/\mu$	36	36	36
Damköhler number, $Da = (l/u')/\tau_c$	0.39	0.48	0.58
Karlovitz number, $Ka = \tau_c/t_\eta$	13.78	11.0	9.20

The Kolmogorov time scale is given by t_η.

due to variations in δ_L, as evident from Table 1. For all three cases the Karlovitz number is greater than unity ($Ka > 1$) and the flames are well within the thin reaction zones regime, and that for the present values of u'/S_L and l/δ_L the flamelet assumption remains valid [9,25]. It can be seen from Table 2 that in all three cases the Damköhler number based on Peters' definition [9] is less than unity, which indicates that strain rate effects on flame propagation are likely to be more important than for $Da > 1$, as indicated by Rutland and Trouvé [8].

Ideally a premixed combustion DNS should be run for a time $t_{lim} = \max(\tau_{f0}, \tau_c)$, where τ_{f0} is the initial eddy turn-over time given by $\tau_{f0} = l/u'$ and τ_c is the chemical timescale defined as $\tau_c = \delta_Z/S_L$ where δ_Z is the flame thickness defined in terms of diffusivity D and laminar burning velocity S_L as $\delta_Z \approx D/S_L$. Here, for the case of $Le = 0.8$, one chemical time corresponds to 2.5 initial eddy turn-over times. The statistics presented below were collected at a time corresponding to $2.5\tau_{f0}$ for all three Lewis number cases. It is recognised that the total simulation time remains small but is consistent with previous combustion DNS studies [6,16,17,26].

It is clear from Eqs. (3), (4) and (9) that temperature plays an important role in displacement speed behaviour, since both reaction rate and density depend strongly on temperature. The joint pdf of temperature and curvature on the $c = 0.8$ isosurface is presented in Fig. 1a and b for $Le = 0.8$ and 1.2 respectively. In the present study this isosurface lies close to the location of maximum reaction rate and hence may be taken as a good marker for the flame location [17,27,28]. It is evident from Fig. 1 that temperature and curvature are positively correlated in the case of $Le = 0.8$ whereas the correlation is negative for $Le = 1.2$. This is consistent with earlier findings from both two-dimensional and three-dimensional compressible and incompressible DNS [5,8,10,15].

The joint pdfs of tangential strain rate and curvature on the $c = 0.8$ isosurface are shown in Fig. 2a–c for the three Lewis number cases considered here. It can be seen clearly that tangential strain rate is negatively correlated with curvature for all three Lewis number cases. This is in agreement with previous findings from DNS [6,27,28] and experiment [29]. The negative correlation between tangential

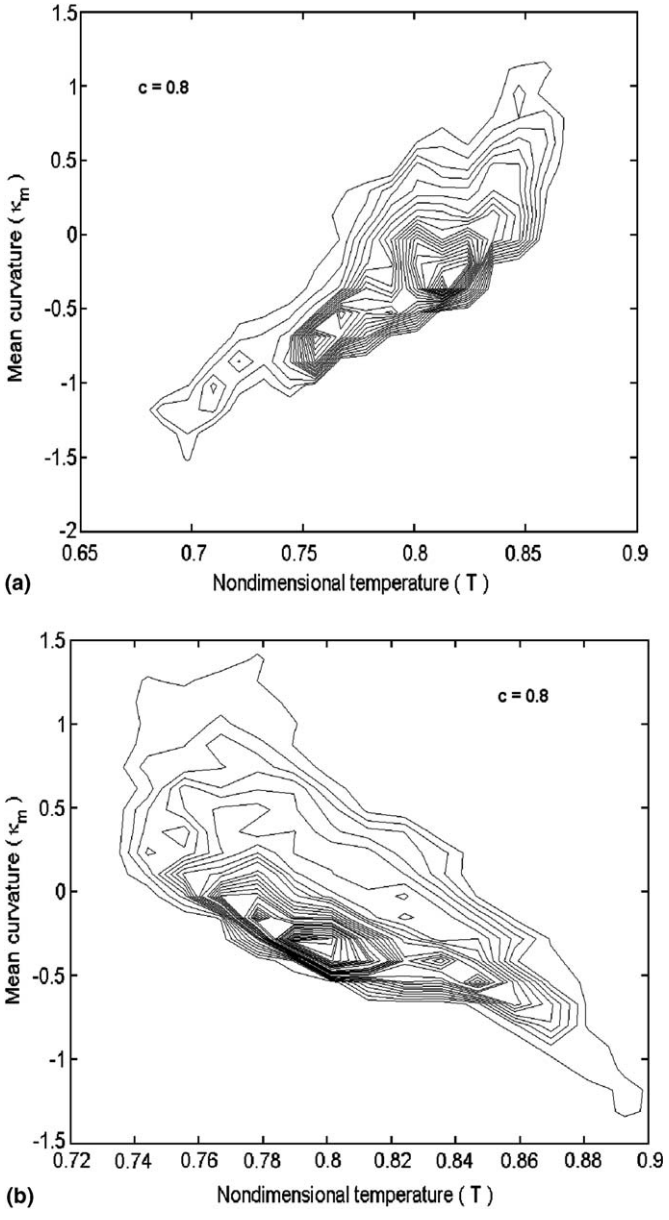

Fig. 1. Joint pdf of non-dimensional temperature and mean curvature on the $c = 0.8$ isosurface: (a) $Le = 0.8$; (b) $Le = 1.2$. Mean curvature is normalised by $1/\delta_L$ corresponding to the respective Lewis number cases.

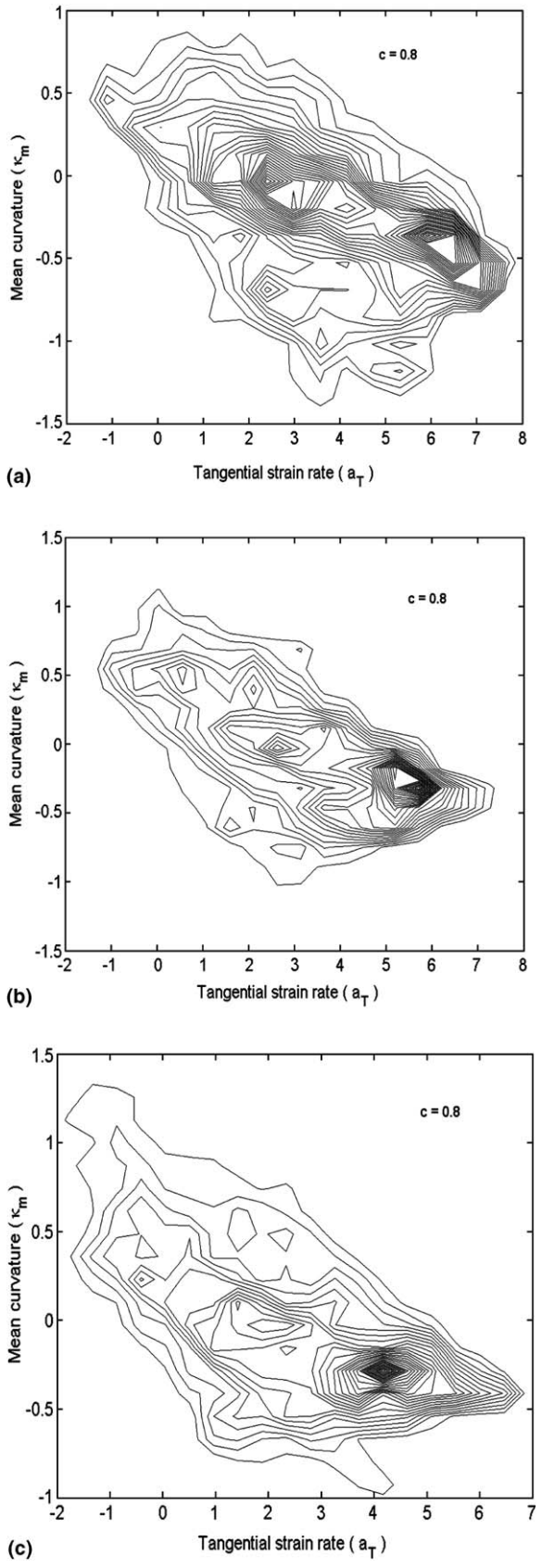

Fig. 2. Joint pdf of tangential strain rate and mean curvature on the $c = 0.8$ isosurface: (a) $Le = 0.8$; (b) $Le = 1.0$; (c) $Le = 1.2$. Tangential strain rate is normalised here and in subsequent figures by S_L/δ_L corresponding to the respective Lewis number cases.

strain rate and curvature is predominantly an effect of heat release and plays an important role in the response of displacement speed to tangential strain rate. It should be noted that previous DNS without heat release did not find a correlation between tangential strain rate and curvature [30,31]. The explanation for this behaviour is that streamline divergence in front of positively curved regions of the flame induces an increased normal strain rate. Moreover defocusing of heat in the positively curved regions gives rise to a lower value of dilatation ($\nabla \cdot \vec{u}$). Since dilatation is the sum of tangential and normal strain rate ($\nabla \cdot \vec{u} = a_T + a_n$), a lower value of dilatation and an increased value of normal strain rate leads to a smaller value of tangential strain rate in positively curved regions, and vice versa.

The joint pdfs of temperature and tangential strain rate are presented in Fig. 3a and b for the Lewis number cases $Le = 0.8$ and 1.2 respectively. For $Le = 0.8$, it is evident that temperature and tangential strain rate are negatively correlated, whereas there is a weak positive correlation for $Le = 1.2$. From Fig. 2a it is clear that for $Le = 0.8$ large positive tangential strain rates are associated with negative values of curvature, which in turn are associated with low values of temperature (see Fig. 1a), leading to the observed negative correlation between temperature and strain rate. The opposite behaviour for $Le = 1.2$ can be explained in the same way with reference to Figs. 1b and 2b. It is important to recognise that the interdependence between tangential strain rate and curvature is manifested implicitly in these correlations. In order to understand the effects of tangential strain rate on temperature in isolation (without the effects of curvature) it is instructive to look at the conditional joint pdfs of temperature and tangential strain rate taken at locations of zero curvature. These are presented in Fig. 3c and d for $Le = 0.8$ and 1.2 respectively. It is found that for $Le = 0.8$, temperature and tangential strain rate are positively correlated whereas a negative correlation is observed for $Le = 1.2$. This is in accordance with previous DNS [8] and the experimental results of Libby et al. [3].

It is clear from Eq. (9) that the local variation of SDF ($|\nabla c|$) on a given c isosurface significantly affects the local displacement speed. The joint pdfs of SDF and tangential strain rate for the three Lewis number cases are presented in Fig. 4, where it is evident that in all three cases SDF and tangential strain rate are positively correlated. This can be explained in terms of the dilatation. It can be shown [27,28] for low Mach number flows that

$$\nabla \cdot \vec{u} = a_T + a_n = \frac{\tau}{(1+\tau T)} \frac{DT}{Dt} \tag{12i}$$

where D/Dt is the total derivative. For Lewis numbers not very different from unity, the right-hand side of Eq. (12) can be scaled as [28]:

$$\frac{\tau}{(1+\tau T)} \frac{DT}{Dt} \sim \tau S_L |\nabla c| \tag{12ii}$$

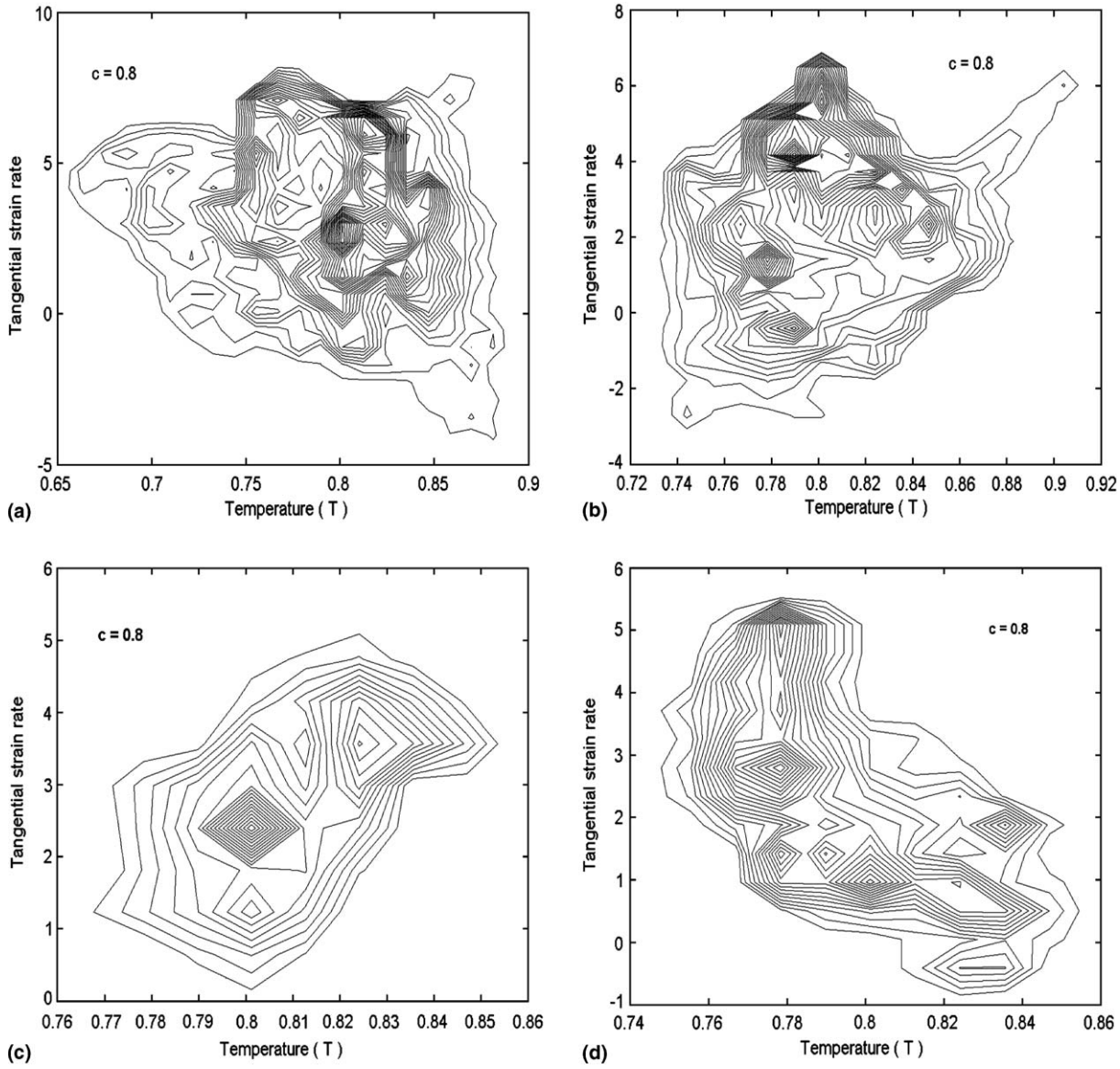

Fig. 3. Joint pdf of non-dimensional temperature and tangential strain rate on the $c = 0.8$ isosurface: (a) $Le = 0.8$; (b) $Le = 1.2$. Conditional joint pdf of non-dimensional temperature and tangential strain rate on the $c = 0.8$ isosurface at zero curvature locations: (c) $Le = 0.8$; (d) $Le = 1.2$.

If the tangential strain rate exceeds the dilatation

$$a_{\mathrm{T}} > \frac{\tau}{(1+\tau T)}\frac{\mathrm{D}T}{\mathrm{D}t} \tag{12iii}$$

which leads to a negative value for a_{n} describing a strain rate that is compressive in nature and which gives rise to a high value of the scalar gradient and hence a high value of SDF. The positive correlation between SDF and tangential strain rate is in agreement with previous three-dimensional DNS at unity Lewis number [28] and will turn out to be a key phenomenon.

The variation of SDF across the flame brush is shown in Fig. 5a–c, where it is evident that in all three Lewis number cases the highest value of SDF is found slightly towards the burned gas side of the flame ($c \approx 0.65$), which is consistent with previous DNS [7,26–28] and experimental results [32–34]. The pdfs of tangential strain rate for all three Lewis number cases are shown in Fig. 5d–f, and the observed behaviour is found to be consistent with previous DNS results [3,8]. For all three Lewis number cases it is clear that the probability of finding positive tangential strain rate is much higher than the probability of finding local negative tangential strain rate. The strain rate pdfs and the SDF scatter from Fig. 5 substantiates that the tangential strain rate a_{T} very often exceeds $\tau S_{\mathrm{L}}|\nabla c|$ as argued in the context of SDF–strain rate correlation.

The joint pdfs of local displacement speed and tangential strain rate for the three Lewis numbers are presented in Fig. 6a–c where it is evident that in all three cases there is a weak correlation. Nevertheless the effects of curvature are implicitly present, and hence it is instructive to look at the corresponding conditional joint pdfs at zero curvature locations. These are shown in Fig. 6d–f, and it is evident that S_{d} and a_{T} are negatively correlated for all three Lewis

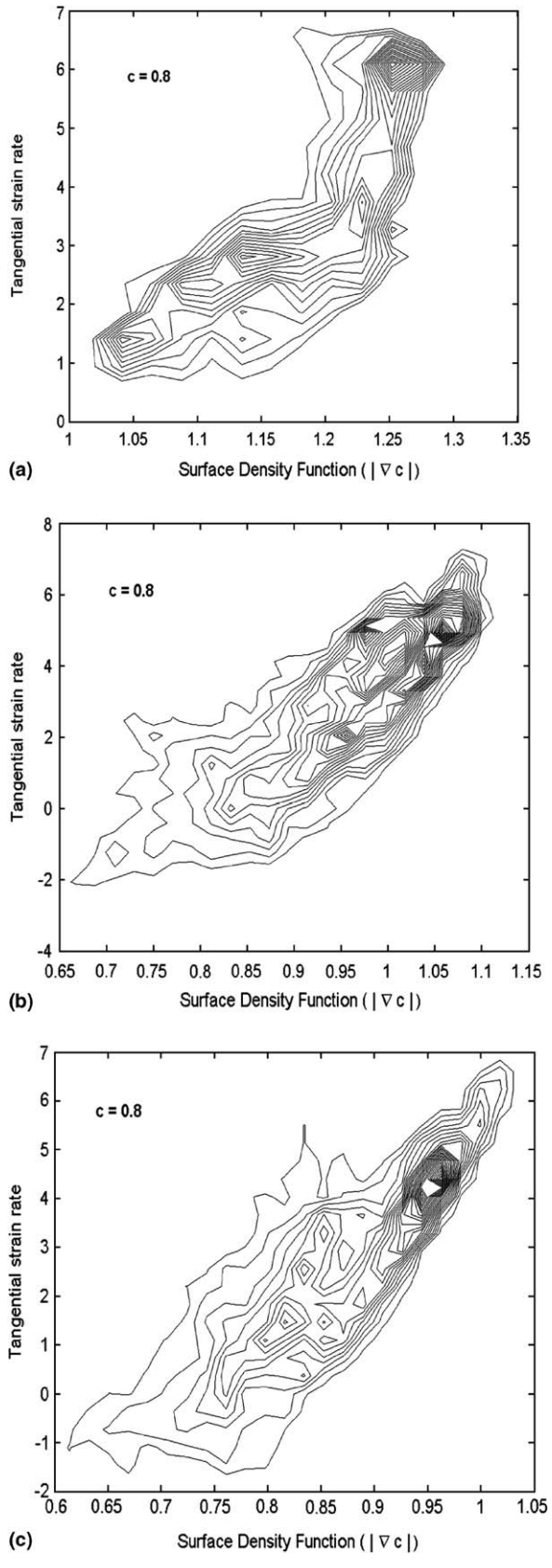

Fig. 4. Joint pdf of SDF ($|\nabla c|$) and tangential strain rate on the $c = 0.8$ isosurface: (a) $Le = 0.8$; (b) $Le = 1.0$; (c) $Le = 1.2$. SDF is normalised with respect to $1/\delta_L$ corresponding to respective Lewis number cases.

number cases. This is consistent with laminar flame theory [9] as well with previous two-dimensional and three-dimensional DNS studies [16,17,27]. It can be seen from Eq. (9iii) that the tangential diffusion component of displacement speed S_t is identically zero at zero curvature locations, so the conditional joint pdf essentially describes the behaviour of $(S_r + S_n)$ with respect to tangential strain rate. This confirms the argument of Peters [9] that $(S_r + S_n)$ contains the strain rate information, and implies that a model for $(S_r + S_n)$ should include strain rate effects in order to address flame propagation behaviour in the thin reaction zones regime.

The behaviour of the different components of displacement speed (S_r, S_n and S_t) is of interest in order to explain the observed weak correlation between displacement speed and tangential strain rate (Fig. 6a–c). The joint pdfs of S_r and tangential strain rate are presented in Fig. 7a–c for $Le = 0.8$, 1.0 and 1.2 respectively. It is clear from Fig. 7a that S_r is negatively correlated with tangential strain rate for $Le = 0.8$. It was shown in Fig. 3a that for $Le = 0.8$ the local temperature and tangential strain rate are negatively correlated, which causes the reaction rate to decrease and the density to increase with increasing tangential strain rate. This results in a negative correlation between the reaction rate per unit mass $(\dot{w}/\rho)$ and tangential strain rate. Since SDF ($|\nabla c|$) increases with tangential strain rate, it also tends to decrease S_r. As a result of these two mechanisms S_r and a_T are negatively correlated in the case of $Le = 0.8$ (see Fig. 7a). In the case of unity Lewis number, $(\dot{w}/\rho)$ remains uniform on a given c isosurface, but the positive correlation between SDF and tangential strain rate produces a negative correlation between S_r and tangential strain rate, as evident from Fig. 7b. In the case of $Le = 1.2$, the local temperature is weakly positively correlated with tangential strain rate which acts to increase $(\dot{w}/\rho)$ with tangential strain rate, but the positive correlation between SDF and tangential strain rate opposes this effect. The competition between these two counter-acting mechanisms results in a weak correlation between S_r and tangential strain rate (see Fig. 7c).

It is evident that for all three Lewis number cases the positive correlation between SDF and tangential strain rate tends to decrease S_r. In the case of $Le = 0.8$ this effect is opposed by the positive correlation between temperature and tangential strain rate at zero curvature locations (Fig. 3c). The temperature–strain rate correlation is the stronger, and the positive correlation between S_r and tangential strain rate prevails at the zero curvature locations, as evident in Fig. 7d. In the case of $Le = 1.2$, at zero curvature locations the temperature is negatively correlated with tangential strain rate (Fig. 3d), which leads to a negative correlation between the conditional reaction rate and tangential strain rate and hence to a negative correlation between S_r and tangential strain rate at zero curvature locations as apparent from Fig. 7f. For the $Le = 1.0$ case the positive correlation between SDF and tangential strain

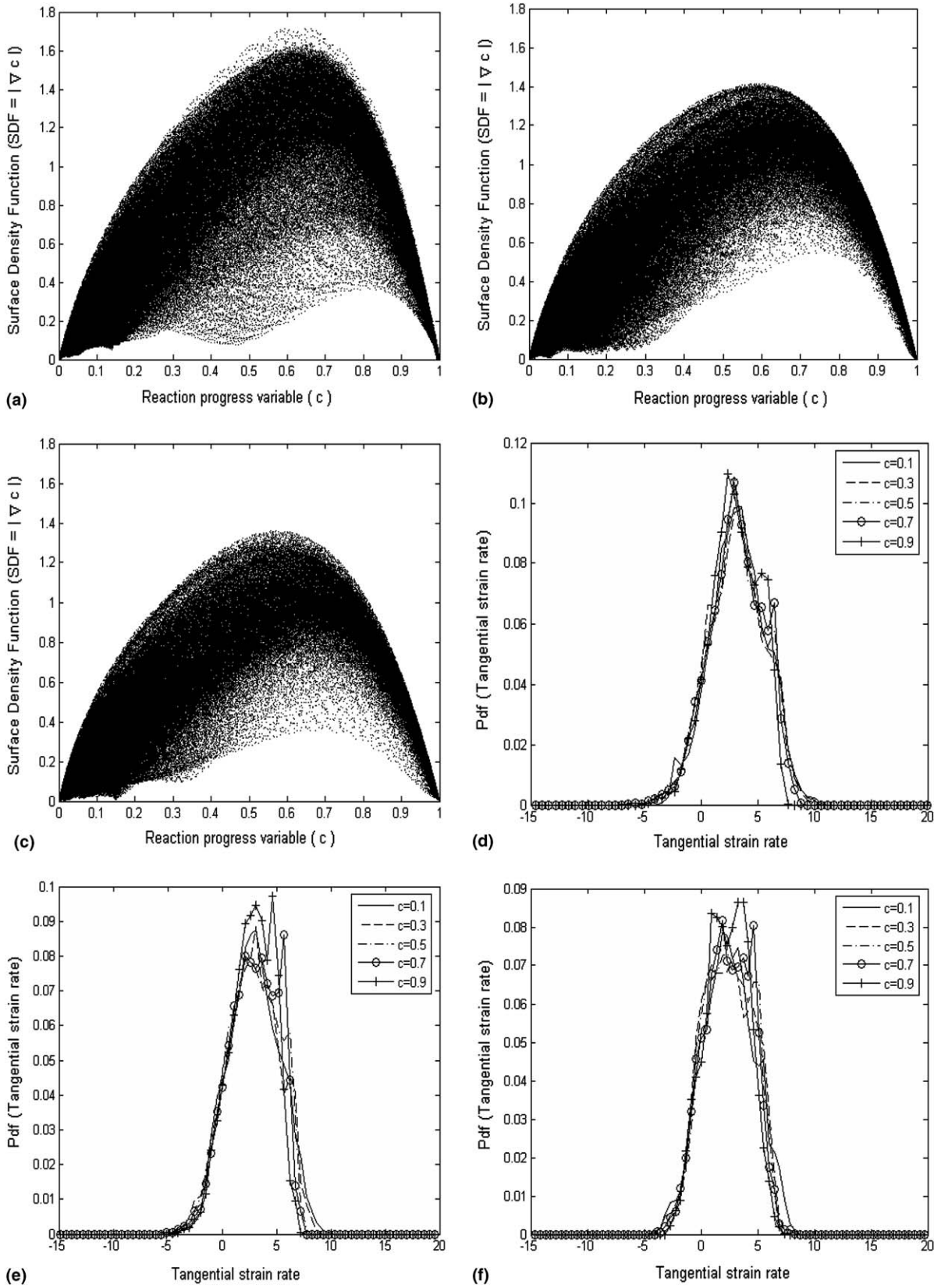

Fig. 5. Scatter of SDF normalised by $(1/\delta_L)$ over the flame brush: (a) $Le = 0.8$; (b) $Le = 1.0$; (c) $Le = 1.2$. Pdfs of tangential strain rate on isosurfaces of progress variable: (d) $Le = 0.8$; (e) $Le = 1.0$; (f) $Le = 1.2$. In the plots the progress variable runs from $c = 0.1$ to 0.9 in steps of 0.2.

rate is entirely responsible for the negative correlation observed between S_r and tangential strain rate at zero curvature locations. These results are in agreement with the experimental findings of Libby et al. [3].

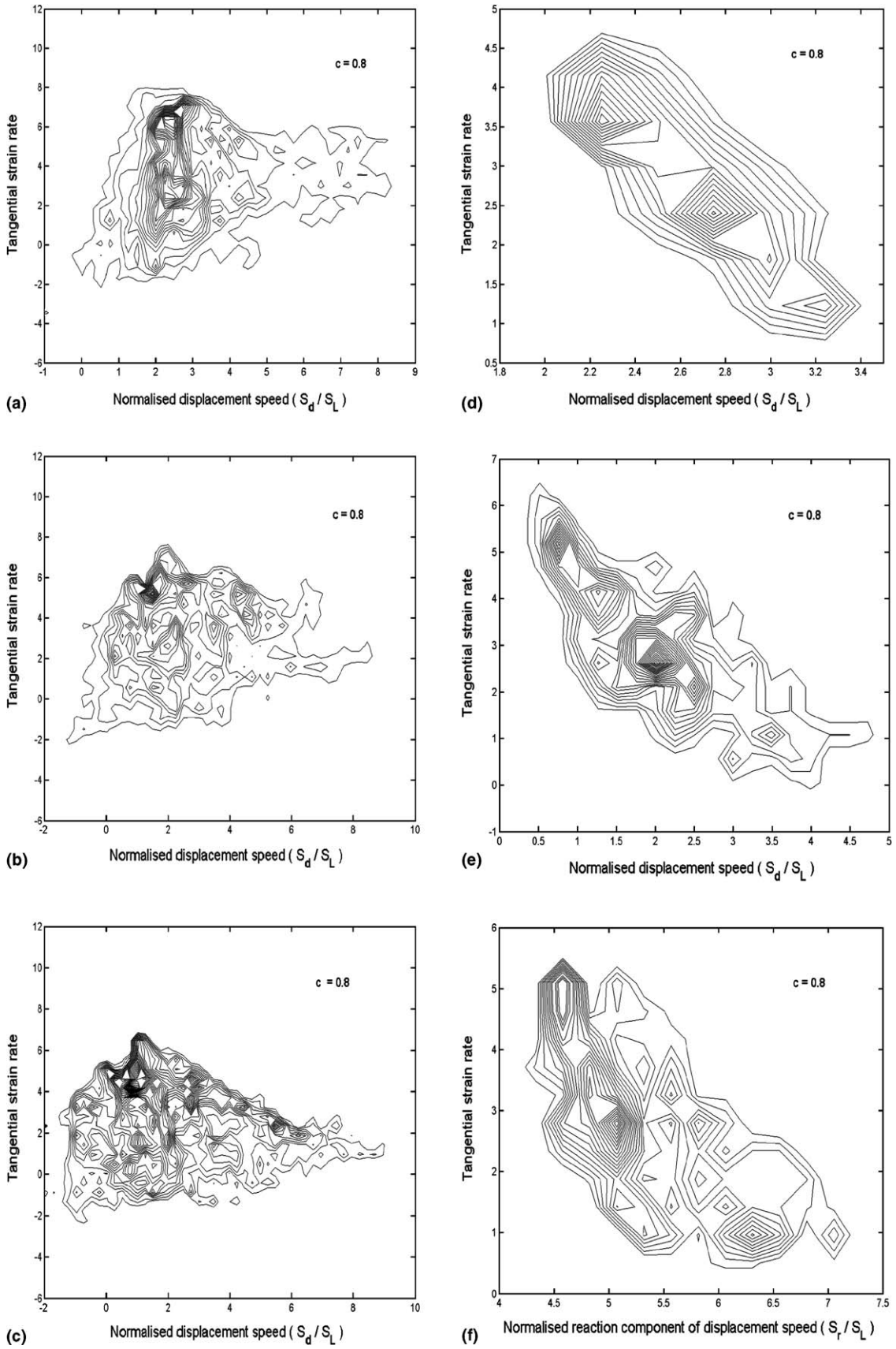

Fig. 6. Joint pdf of normalised displacement speed (S_d) and tangential strain rate on the $c = 0.8$ isosurface: (a) $Le = 0.8$; (b) $Le = 1.0$; (c) $Le = 1.2$. Conditional joint pdf of S_d and tangential strain rate on the $c = 0.8$ isosurface at zero curvature locations: (d) $Le = 0.8$; (e) $Le = 1.0$; (f) $Le = 1.2$. In this and subsequent figures the displacement speed and its components are normalised by the unstrained laminar flame speed S_L.

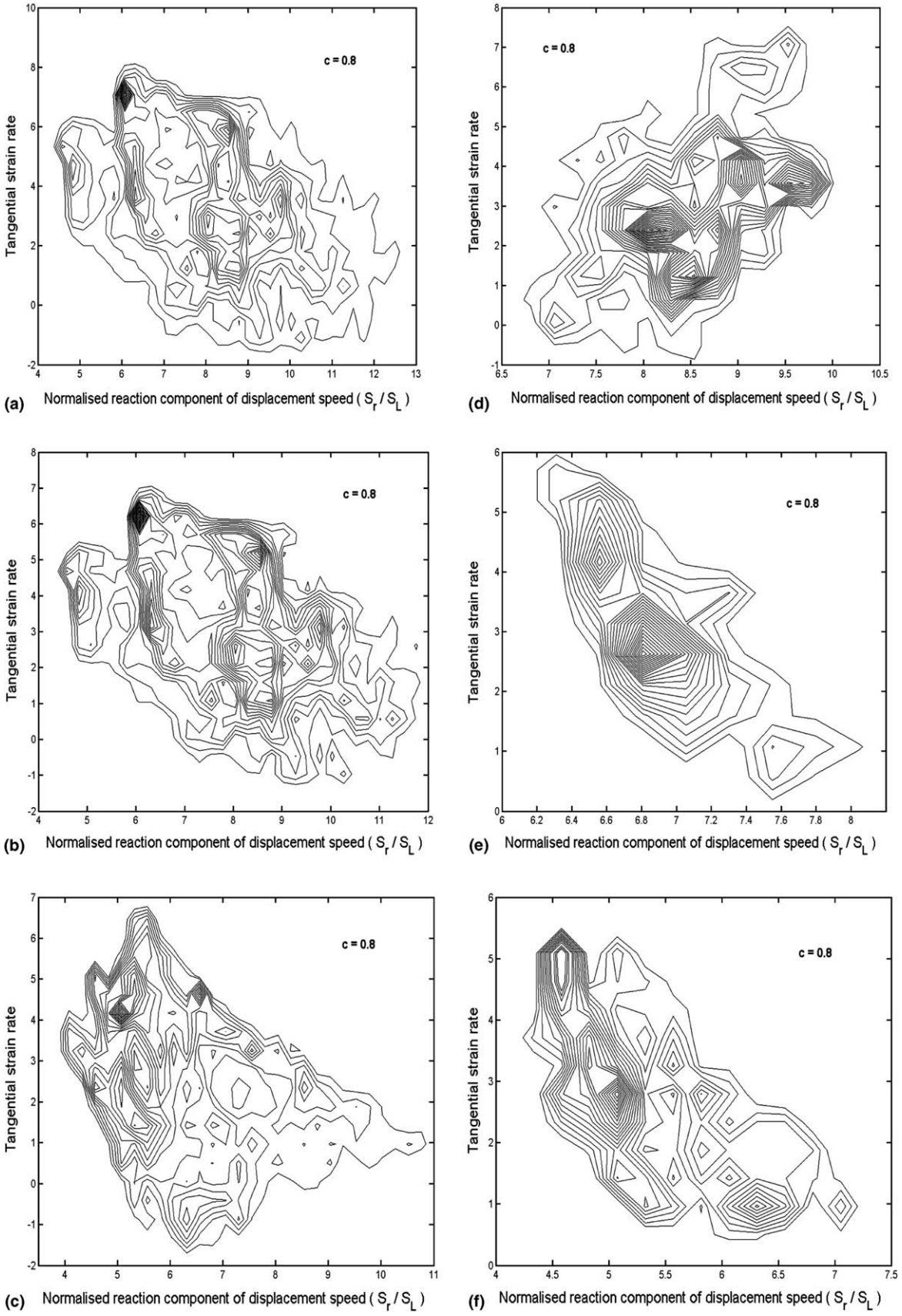

Fig. 7. Joint pdf of normalised reaction component of displacement speed (S_r) and tangential strain rate on $c = 0.8$ isosurface: (a) $Le = 0.8$; (b) $Le = 1.0$; (c) $Le = 1.2$. Conditional joint pdf of S_r and tangential strain rate on the $c = 0.8$ isosurface at zero curvature locations: (d) $Le = 0.8$; (e) $Le = 1.0$; (f) $Le = 1.2$.

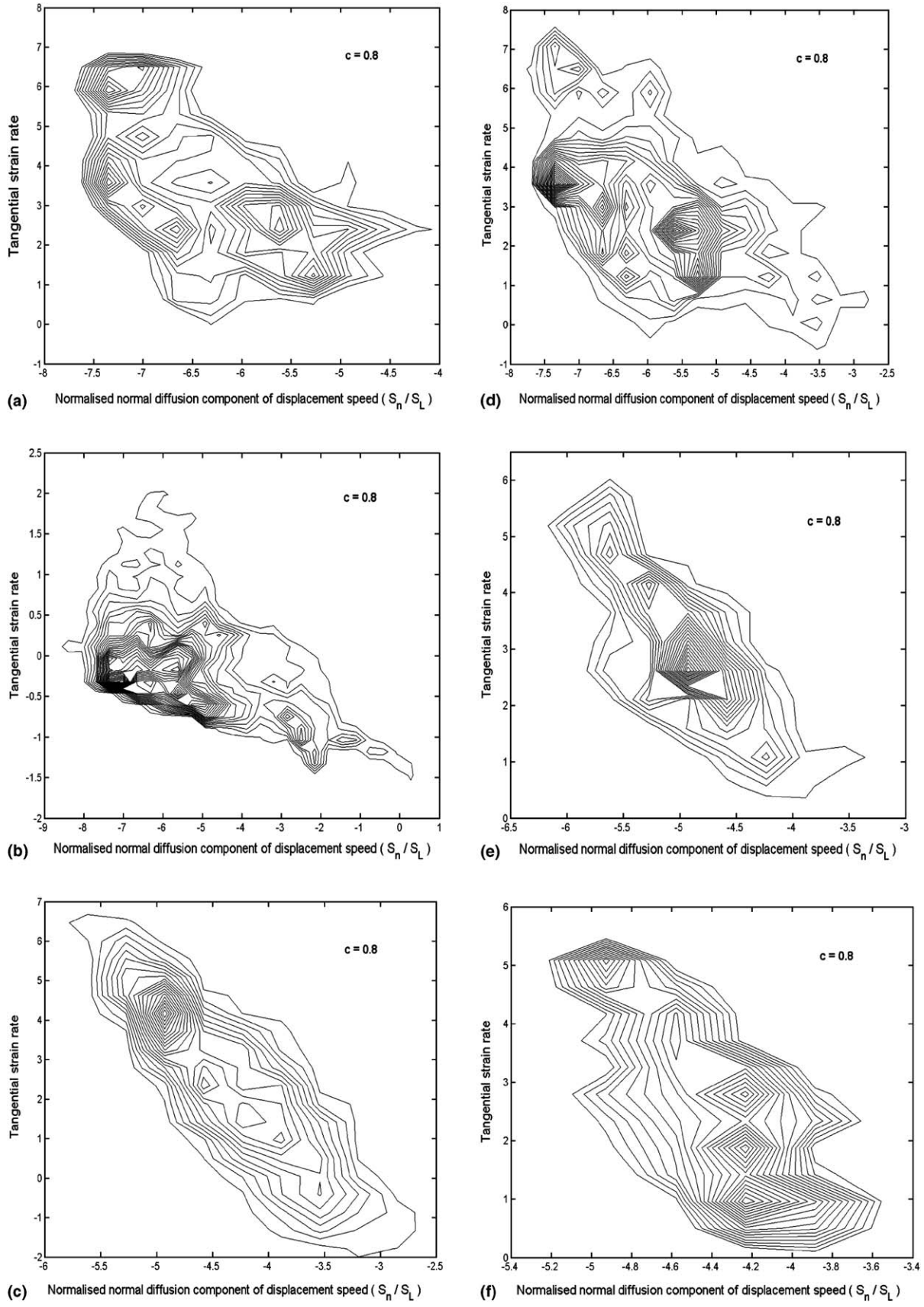

Fig. 8. Joint pdf of normalised normal diffusion component of displacement speed (S_n) and tangential strain rate on the $c = 0.8$ isosurface: (a) $Le = 0.8$; (b) $Le = 1.0$; (c) $Le = 1.2$. Conditional joint pdf of S_n and tangential strain rate on the $c = 0.8$ isosurface at zero curvature locations: (d) $Le = 0.8$; (e) $Le = 1.0$; (f) $Le = 1.2$.

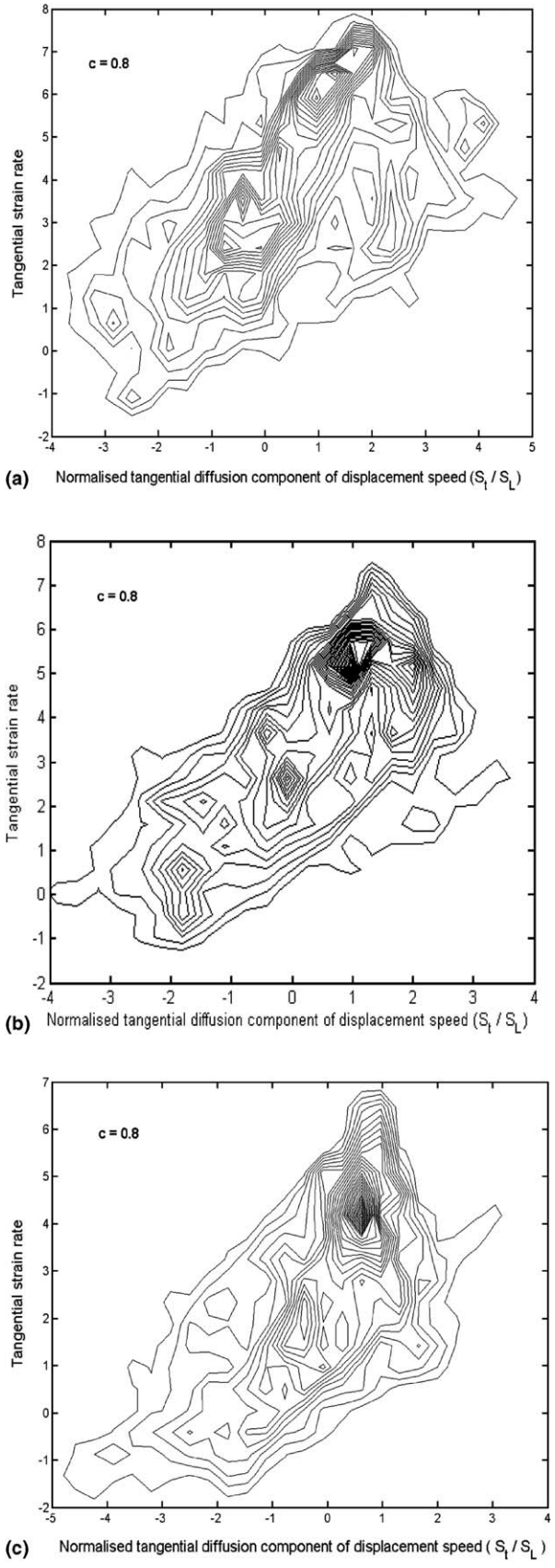

Fig. 9. Joint pdf of normalised tangential diffusion component of displacement speed (S_t) and tangential strain rate on the $c = 0.8$ isosurface: (a) $Le = 0.8$, (b) $Le = 1.0$, (c) $Le = 1.2$.

The reciprocal of SDF ($|\nabla c|$) can be taken as a measure of local flame thickness δ, and so the positive correlation between SDF and tangential strain rate implies that δ decreases with increasing tangential strain rate. The normal diffusion rate $\vec{N} \cdot \nabla(\rho D \vec{N} \cdot \nabla c)$ in the reaction zone scales as $(-\rho D \delta^{-2})$ whereas the SDF itself scales as δ^{-1}. As a result of this, S_n (see Eq. (9iv)) varies with δ as $(-D\delta^{-1})$. An increase in tangential stain rate decreases δ, which eventually decreases $(-D\delta^{-1})$ as well. This is reflected in the negative correlation observed between S_n and tangential strain rate for all three Lewis number cases (see Fig. 8a–c), and the same physical mechanism is also valid for the corresponding zero curvature conditional joint pdfs (see Fig. 8d–f).

The joint pdfs of the tangential diffusion component S_t and tangential strain rate are presented in Fig. 9a–c for the three Lewis numbers, and all show a positive correlation. Since S_t is proportional to the negative of local curvature (Eq. (9iii)), and since curvature and tangential stain rate are negatively correlated, S_t is positively correlated with tangential strain rate and this opposes the effects of the negative correlation between $(S_r + S_n)$ and tangential strain rate. As a result, local displacement speed S_d does not show any appreciable correlation with local tangential strain rate. This clearly demonstrates the indirect effects of curvature on the strain rate response of displacement speed in the thin reaction zones regime.

It has been shown analytically by Joulin [35] that for high frequency perturbations the effect of strain rate disappears. DNS studies by Chen and Im [17] and Chakraborty and Cant [28] confirmed that the correlation between S_d and a_T decreases with increasing turbulence fluctuation level. This study also shows weak correlation between local S_d and a_T. Strain rate effects on displacement speed are expected to be much weaker for very high turbulence intensities when flame approaches the broken reaction zones regime. The conditions at which the Lewis number effects on the correlation between displacement speed and tangential strain rate disappear will be addressed in future studies.

5. Conclusions

The present study leads to a number of important conclusions which are summarised below:

1. The correlation between temperature and curvature affects the strain rate response of temperature through the correlation between tangential strain rate and curvature. The temperature-curvature correlation is positive (negative) for the $Le = 0.8$ ($Le = 1.2$) case. For the unity Lewis number case, the temperature remains uniform on a given reaction progress variable isosurface. The correlation between tangential strain rate and curvature is found to be negative for all Lewis numbers considered here which is consistent with previous DNS and experimental results [6,26–28].

2. The correlation between temperature and strain rate is positive at zero curvature locations for the $Le = 0.8$ case. By contrast, this correlation is negative for the $Le = 1.2$ case. This is in agreement with previous experimental results from stagnation point flames [8].
3. It is shown that for all cases considered here the SDF and tangential strain rate are positively correlated which indicates that the local flame thickness decreases with increasing tangential strain rate.
4. The combined effects of the local temperature–strain rate and SDF–strain rate correlations lead to a negative correlation between the reaction component of displacement speed S_r and tangential strain rate for the $Le = 0.8$ case. This correlation is weak for the $Le = 1.2$ case. A positive SDF–strain rate correlation leads to a negative correlation between S_r and tangential strain rate for the unity Lewis number case.
5. The conditional joint pdf between S_r and tangential strain rate at zero curvature locations shows a positive correlation for the $Le = 0.8$ case and a negative correlation for the $Le = 1.2$ case. Flame thinning associated with high values of tangential strain rate leads to a negative correlation between S_r and tangential strain rate for the unity Lewis number case.
6. Local flame thinning in response to high values of tangential strain rate leads to a negative correlation between the normal diffusion component of displacement speed S_n and tangential strain rate in the reaction zone for all Lewis number cases considered here.
7. A weak correlation is observed between local displacement speed S_d and tangential strain rate. However, the conditional joint pdf of S_d and tangential strain rate at zero curvature locations reveals a negative correlation. Previous two-dimensional DNS with detailed chemistry [16,17] revealed similar qualitative behaviour, which is captured in the present study even in the absence of detailed chemistry and is due purely to the fluid-dynamical aspects of the flame-turbulence interaction. At zero curvature locations, the tangential diffusion component of displacement speed S_t is identically zero, which indicates that the conditional joint pdf of S_d and tangential strain rate at zero curvature locations is essentially identical to the joint pdf between $(S_r + S_n)$ and tangential strain rate. The joint pdf of the tangential diffusion component of displacement speed S_t and tangential strain rate reveals a positive correlation because of the negative correlation between tangential strain rate and curvature. This indicates that in the absence of additional curvature effects, $(S_r + S_n)$ contains all the strain rate information. This finding confirms the argument of Peters [9] for the modelling of displacement speed in the thin reaction zones regime.
8. As $(S_r + S_n)$ and tangential strain rate are correlated, it is necessary to take strain rate effects into account in the modelling of $(S_r + S_n)$. In addition, strain rate effects appear indirectly through the correlation between tangential strain rate and curvature which also needs to be accounted for in the modelling framework. This is of particular importance in the context of large eddy simulation (LES).

In the present study, the response of turbulent premixed flame propagation to variations in tangential strain rate is correctly captured using simplified chemistry by accounting for differential diffusion effects. Based on the agreement between two-dimensional detailed chemistry DNS and three-dimensional simple-chemistry DNS, it is unlikely that three-dimensional DNS with detailed chemistry would reveal any radically new behaviour. However the present findings are mainly of qualitative importance. For quantitative analysis, three-dimensional DNS with detailed chemistry is still a requirement for future work.

References

[1] P. Clavin, F.A. Williams, Effects of molecular diffusion and thermal expansion on the structure and dynamics of turbulent premixed flames in turbulent flows of large scale and small intensity, J. Fluid Mech. 116 (1982) 251–282.
[2] G.I. Sivashinsky, Diffusional-thermal theory of cellular flames, Combust. Sci. Technol. 15 (1977) 137–146.
[3] P.A. Libby, A. Linan, F.A. Williams, Strained premixed laminar flames with non-unity Lewis numbers, Combust. Sci. Technol. 34 (1983) 257–293.
[4] R.G. Abdel-Gayed, D. Bradley, M. Hamid, M. Lawes, Lewis number effects on turbulent burning velocity, Proc. Combust. Inst. 20 (1984) 505–512.
[5] W.T. Ashurst, N. Peters, M.D. Smooke, Numerical simulation of turbulent flame structure with non-unity Lewis number, Combust. Sci. Technol. 53 (1987) 339–375.
[6] D.C. Haworth, T.J. Poinsot, Numerical simulations of Lewis number effects in turbulent premixed flames, J. Fluid Mech. 244 (1992) 405–436.
[7] A. Trouvé, T. Poinsot, The evolution equation for flame surface density in turbulent premixed combustion, J. Fluid Mech. 278 (1994) 1–31.
[8] C.J. Rutland, A. Trouvé, Direct simulations of premixed turbulent flames with nonunity Lewis numbers, Combust. Flame 94 (1993) 41–57.
[9] N. Peters, Turbulent Combustion, first ed., Cambridge University Press, UK, 2000, pp. 66–169.
[10] H.G. Im, J.H. Chen, Preferential diffusion effects on the burning rate of interacting turbulent premixed hydrogen-air flames, Combust. Flame 126 (2002) 246–258.
[11] T. Shamim, The effect of Lewis number on radiative extinction and flamelet modelling, Int. J. Heat Mass Transfer 45 (2002) 1249–1259.
[12] R. Hilbert, D. Thévenin, Influence of differential diffusion on maximum flame temperature in turbulent nonpremixed hydrogen/air flames, Combust. Flame 138 (2004) 175–187.
[13] S.B. Pope, The evolution of surfaces in turbulence, Int. J. Engng. Sci. 26 (5) (1988) 445–469.
[14] S.M. Candel, T.J. Poinsot, Flame stretch and the balance equation for the flame area, Combust. Sci. Technol. 70 (1990) 1–15.
[15] N. Chakraborty, R.S. Cant, Influence of Lewis number on curvature effects in turbulent premixed flame propagation in the thin reaction zones regime, Phys. Fluids 17 (2005) 10105-1–10105-20.
[16] T. Echekki, J.H. Chen, Unsteady strain rate and curvature effects in turbulent premixed methane-air flames, Combust. Flame 106 (1996) 184–202.

[17] J.H. Chen, H.G. Im, Stretch effects on the burning velocity of turbulent premixed hydrogen/air flames, Proc. Combust. Inst. 28 (2000) 211–218.
[18] N. Peters, P. Terhoeven, J.H. Chen, T. Echekki, Statistics of flame displacement speeds from computations of 2-D unsteady methane-air flames, Proc. Combust. Inst. 27 (1998) 833–839.
[19] W. Kollmann, J.H. Chen, Pocket formation and the flame surface density equation, Proc. Combust. Inst. 27 (1998) 927–934.
[20] T. Poinsot, S.K. Lele, Boundary conditions for direct simulation of compressible viscous flows, J. Comput. Phys. 101 (1992) 104–129.
[21] G.K. Batchelor, A.A. Townsend, Decay of turbulence in final period, Proc. Roy. Soc. A 194 (1948) 527–542.
[22] R.S. Rogallo, Numerical experiments in homogeneous turbulence, NASA TM81315, NASA Ames Research Center, California, 1981.
[23] K.W. Jenkins, R.S. Cant, DNS of turbulent flame kernels, in: Proc. Second AFOSR Conf. on DNS and LES, Kluwer Academic Publishers, 1999, pp. 192–202.
[24] A.A. Wray, Minimal storage time advancement schemes for spectral methods, unpublished report, NASA Ames Research Center, California, 1990.
[25] T. Poinsot, D. Veynante, S. Candel, Quenching processes and premixed turbulent combustion diagrams, J. Fluid Mech. 228 (1991) 561–606.
[26] M. Boger, D. Veynante, H. Boughanem, A. Trouvé, Direct numerical simulation analysis of flame surface density concept for large eddy simulation of turbulent premixed combustion, Proc. Combust. Inst. 27 (1998) 917–925.
[27] N. Chakraborty, S. Cant, Unsteady effects of strain rate and curvature on turbulent premixed flames in an inflow–outflow configuration, Combust. Flame 137 (2004) 129–147.
[28] N. Chakraborty, R.S. Cant, Effects of strain rate and curvature on surface density function transport in turbulent premixed flames in the thin reaction zones regime, Phys. Fluids A 17 (2005) 65108-1–65108-15.
[29] B. Renou, A. Boukhalfa, D. Peuchberty, M. Trinité, Effects of stretch on the local structure of freely propagating premixed low-turbulent flames with various Lewis numbers, Proc. Combust. Inst. 27 (1998) 841–847.
[30] R.S. Cant, C.J. Rutland, A. Trouvé, Statistics for laminar flamelet modelling, in: Proceeding of the Summer Program 1990, Center for Turbulence Research, Stanford, 1990, pp. 271–279.
[31] R.S. Cant, Direct numerical simulation of premixed turbulent flames, Philos. Trans. Roy. Soc. Lond. A 357 (1999) 3583–3604.
[32] J.F. Driscoll, A. Gulati, Measurement of various terms in turbulent kinetic balance within a flame and comparison with theory, Combust. Flame 72 (1988) 131–152.
[33] R.K. Cheng, I.G. Shepherd, L. Talbot, Reaction rates in premixed turbulent flames and their relevance to turbulent burning speed, Proc. Combust. Inst. 22 (1988) 771–780.
[34] T.C. Chew, K.N.C. Bray, R.E. Britter, Spatially resolved flamelet statistics for reaction rate modelling, Combust. Flame 80 (1990) 65–82.
[35] G. Joulin, On the response of premixed flames to time-dependent stretch and curvature, Combust. Sci. Technol. 97 (1994) 219–229.